

## Effect of biaxial strain on half-metallicity of transition metal alloyed zinc-blende ZnO and GaAs: a first-principles study

This article has been downloaded from IOPscience. Please scroll down to see the full text article.

2011 J. Phys. D: Appl. Phys. 44 205002

(<http://iopscience.iop.org/0022-3727/44/20/205002>)

View [the table of contents for this issue](#), or go to the [journal homepage](#) for more

Download details:

IP Address: 222.201.152.89

The article was downloaded on 23/05/2011 at 02:11

Please note that [terms and conditions apply](#).

# Effect of biaxial strain on half-metallicity of transition metal alloyed zinc-blende ZnO and GaAs: a first-principles study

Li-Juan Chen, Ren-Yu Tian, Xiao-Bao Yang and Yu-Jun Zhao

Department of Physics, South China University of Technology, Guangzhou 510640, People's Republic of China

E-mail: [zhaoyj@scut.edu.cn](mailto:zhaoyj@scut.edu.cn)

Received 20 January 2011, in final form 28 March 2011

Published 3 May 2011

Online at [stacks.iop.org/JPhysD/44/205002](http://stacks.iop.org/JPhysD/44/205002)

## Abstract

The electronic structure, magnetic and half-metallic properties of transitional metal (TM)-alloyed zinc-blende ZnO and GaAs (TM = Cr, Mn, Fe, Co, Ni) thin films with biaxial strains on the (001) plane are studied by density functional theory and beyond. Here, we focus on two simple layer-by-layer delta doping structures with the TM substituting along the (100) planes (type-I) and (001) planes (type-II). We find that the Fe-, Co- and Ni-alloyed GaAs, Mn- and Fe-alloyed ZnO, and Co-alloyed ZnO(II) show antiferromagnetic (AFM) states, while Ni-alloyed ZnO(I) and Cr-alloyed GaAs show ferromagnetic (FM) coupling independent of the biaxial strain within 25% along the (001) plane. For the systems of Cr-alloyed ZnO, Co-alloyed ZnO(I), Ni-alloyed ZnO(II) and Mn-alloyed GaAs(I, II), the strain from the substrate will induce a phase transition from AFM to FM states. The Co-alloyed ZnO(I), Ni-alloyed ZnO(I, II) and Cr-alloyed GaAs(I, II) systems are demonstrated to be half-metallic from the generalized gradient approximation (GGA) calculations. The Cr-alloyed ZnO and Mn-alloyed GaAs systems also show robust half-metallicity with a large spin-flip gap by a GGA +  $U$  description, although their half-metallicity disappears with the standard GGA description.

(Some figures in this article are in colour only in the electronic version)

## 1. Introduction

The ongoing demand of spintronic materials allowing the manipulation of both charge and spin freedoms in a single material has driven extensive theoretical and experimental studies in transition metal (TM) doping and interface physics in semiconductors. Most research groups focus on two aspects of spintronic material study [1]. One is the diluted magnetic semiconductors (DMSs) which are non-magnetic semiconductors doped with TM elements to possess the intermediate properties between non-magnetic semiconductors and magnetic metals [2, 3]. TM-doped II–VI or III–V semiconductors are the most frequently studied systems, particularly Co- or Mn-doped ZnO, in which room-temperature ferromagnetism (RTFM) was predicted theoretically by Dietl and Sato [4, 5]. The other one is half-metallic ferromagnets (HMFs) which may be fabricated by

an advanced interface technique for an efficient injection of spin-polarized carriers into semiconductors [6–11]. Some experimental studies on HMF have been conducted in recent years [12, 13]. For example, Mansell and his group have presented a series of measurements on a molecular beam epitaxy (MBE)-grown half-metallic  $\text{Fe}_3\text{O}_4:\text{Al}_{0.1}\text{Ga}_{0.9}\text{As}$  device with spin-selective injection across the interface [13]. Meanwhile, many theoretical studies showed that most of the early TM pnictides and chalcogenides in the metastable zinc-blende (ZB) structure are half-metallic when they maintain a relatively large lattice constant, or are grown on a semiconductor substrate with sufficiently large lattice constants. A recent theoretical study has even found that the ZB CrTe (001) *surface* shows a robust half-metallicity [14].

Up to now, some theoretical studies and experimental reports have shown that RTFM could be realized by doping a traditional semiconductor (such as GaN or ZnO with a large

band gap) with magnetic elements [15–19]. The origin of FM ordering in these systems and even their *feasibility*, however, are still a matter of debate [20, 21]. At the same time, the HMFs also hold a great promise for spintronic applications. This is based on the fact that the spin splitting and, therefore, the spin-flip (SF) gap of these compounds change drastically with volume expansion and compression [22]. Whereas, in nature, these materials are stable in structures other than ZB. Recently, Zhao and Zunger [23] investigated the relative stability of NiAs and ZB structures under pseudomorphic epitaxial conditions. They argued that under epitaxial growth conditions, for most of the Cr and Mn pnictides and chalcogenides, the NiAs structure is always lower in energy than ZB. So far, further theoretical studies on numerous binary alloys (such as Cr-, Mn-, V-pnictides and chalcogenides) have been conducted by some research groups [24–29]. These previous studies have shown that it is also difficult to achieve ZB thin films by epitaxy on available semiconductor substrates with NiAs or ZB structure. In experimental studies, Zhao *et al* have prepared CrAs, CrSb and MnAs super thin films in ZB structure [30–32]. Although these films favour the FM state, they do not maintain half-metallicity due to the boundary or interface effect, which will reduce the efficiency of injecting spin-polarized carriers into the semiconductor [24].

Meanwhile, assisted by the state-of-the-art MBE technology, it is possible to grow a variety of semiconductor heterostructures controlled atom by atom, and by abrupt doping profiles such as delta doping [33–35]. It has been reported that Mn could be delta doped in ZB GaAs substitutionally within 2–3 monolayers [34]. Furthermore, there are some experimental studies showing that the TM doping ratio could also be high in much thicker films. For example, the Santa Barbara group has reported that reproducible 100 nm thick  $\text{Ga}_{1-x}\text{Mn}_x\text{As}$  films with doping concentration up to  $x = 0.22$  were grown using a combinatorial technique to achieve stoichiometry [36]. Considering the difficulty of acquiring HMF of binary ZB alloys, delta doping of TM by MBE technology in a variety of semiconductors on suitable ZB substrates is an alternative way for efficient spin injection. With appropriate choices of substrate lattice, it is expected that the stability of delta-doped ZB structures of interesting semiconductors, such as GaAs:TM and ZnO:TM could be more robust. Therefore, it is important to understand how the biaxial strain affects the electronic structure and half-metallicity. Here, we have studied the half-metallicity, electronic and magnetic properties of possible ternary alloy films of (Zn, TM)O and (Ga, TM)As (TM = Cr, Mn, Fe, Co, and Ni) under a biaxial strain, assuming that the samples are grown on various semiconductor substrates of conventional ZB structure. We intend to focus on two issues. (i) How the biaxial strain affects the ferromagnetism of the ternary alloy films based on ZnO and GaAs (such as Ga–Mn–As, Ga–Cr–As, Ga–Co–As, Zn–Mn–O, Zn–Cr–O and Zn–Co–O) in ZB structure? (ii) Will the half-metallic property exist in these ternary alloy films? GGA +  $U$  calculations are also conducted in addition to the standard density functional theory (DFT) calculations to involve the strong correlation effect on the systems.

## 2. Computational details

Our theoretical studies are carried out within the framework of DFT combined with GGA. All the calculations are performed with the pseudopotential plane wave method [37] with the PW91 formulae [38], and the projector-augmented wave (PAW) potentials, as implemented in the VASP code [39, 40]. An energy cut-off of 500.0 eV and  $\Gamma$ -centred  $6 \times 6 \times 6$   $k$  meshes for Zn–TM–O and Ga–TM–As, following the Monkhorst–Pack  $k$ -space integration method are employed [41]. In structure search, all cell-internal structural parameters are fully relaxed. The calculation is stopped when forces of all the relaxed atoms are less than  $0.001 \text{ eV } \text{\AA}^{-1}$ . In particular, for the Zn–Cr–O and Ga–Mn–As systems, we have also applied Hubbard- $U$  corrections [42–44] to GGA in order to validate our results on half-metallicity by improving the description of their TM-d states [45–48]. It is not easy to choose proper  $U$  values for the TM in a given environment. To avoid artificial HM property raised by inappropriate high  $U$  values, we employed the  $U$  values of 2.5 eV, 3.0 eV, 3.5 eV and 4.0 eV, 4.5 eV, 4.5 eV for Mn and Cr, respectively. These values are chosen to be close to the corresponding values in a near free electron gas environment, 3.0 eV and 3.9 eV for Mn and Cr, correspondingly (as reported in [44]), which are expected to be smaller than the realistic values in our studied systems.

## 3. Results and discussion

During the epitaxial growth process, the in-plane lattice constants of a film will decrease or increase along with changes in the substrate lattice. According to experiments, the ZB ternary compound prefers to grow along the [001] direction on (001) planes of substrates of ZB structure [49]. Typically, the films prepared in experiments are tens of nanometres in thickness and were often simulated by bulk models with biaxial strains [22, 23, 28]. In our calculations, we fix the lattice constants of the systems along  $a$ - and  $b$ -axes for corresponding substrates and then relax along the  $c$ -axis. The subsequent changes in half-metallicity under the biaxial strain, usually depends on the isotropic strain significantly. Generally, under the epitaxial growth conditions, the stability of a ZB film fabricated in epitaxial growth is not determined by the energy difference  $\Delta_{\text{bulk}}$  between the isotropic deformed ZB materials and the ground state structure but rather by the energetics of the biaxial deformed film relative to the ground state,  $\Delta_{\text{epi}}$  [50]. As for the 50% TM-alloyed GaAs studied here, its ground state structure is not clear, but expected to be similar to that of GaAs or MnAs, i.e. ZB or NiAs type. Here, we studied the NiAs-type and ZB structures of ferromagnetic  $\text{GaMnAs}_2$ , and found that the total energies of these two structures are  $-42.07 \text{ eV}$  and  $-42.81 \text{ eV}$  for a cell of 8 atoms, respectively. This indicates that the ZB structure could be more stable than the NiAs-type structure of  $\text{GaMnAs}_2$ . Meanwhile, there are some occasional experimental reports on ZB GaAs samples grown on substrates with a large lattice mismatch [51]. Therefore, we argue that there are chances to grow TM-alloyed GaAs and ZnO films with ZB on appropriate substrates.

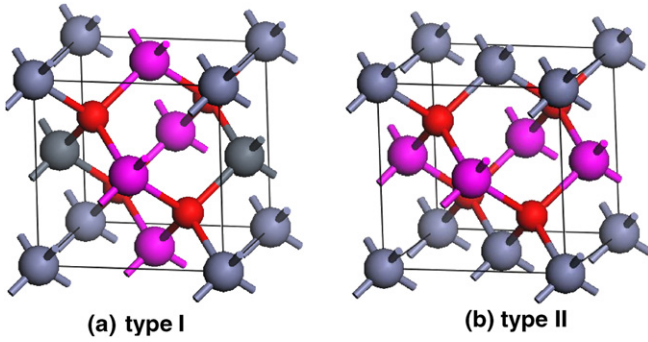


**Figure 1.** The structure of two types of ZB TM-doped ZnO and GaAs. The Zn (Ga), TM (Cr, Mn, Fe, Co, Ni) and O atoms are represented by grey, pink and red balls, respectively.

There are two typical types of structures for the TM-alloyed ZnO or GaAs film with a concentration of 50% in ZB under the biaxial strain ( $c/a \neq 1$ ) (shown in figure 1): (a) one is that the cation atoms are substituted by TM (Mn, Fe, Co, Cr, Ni) on the alternative [100] planes of the film, named type I here; (b) the other is that the cation atoms are substituted by TM on the alternative [001] planes, named type II here.

### 3.1. Magnetism described by the GGA approach

We investigated the strain effect on the magnetic properties and half-metallicity of TM-alloyed ZnO and GaAs films. Figure 2 shows the variation of the  $c/a$  ratio, total energy, magnetization and  $\Delta E$  ( $\Delta E = E_{\text{AFM}} - E_{\text{FM}}$ ) (the total energy difference between AFM and FM states) as a function of strain which is in the range from  $-15\%$  to  $30\%$  of its equilibrium lattice constant  $a_0$ . When the total energy difference  $\Delta E > 0$ , it indicates that the film prefers the FM state, and it prefers the AFM state for  $\Delta E < 0$ . According to our GGA results, the TM-alloyed ZnO and GaAs films are classified into three groups listed in table 1.

The first group corresponds to the systems with their magnetic states changing from the AFM to the FM state when the substrate lattice constant increases, i.e.  $\text{Zn}_{0.5}\text{Cr}_{0.5}\text{O(I,II)}$ ,  $\text{Zn}_{0.5}\text{Co}_{0.5}\text{O(I)}$ ,  $\text{Zn}_{0.5}\text{Ni}_{0.5}\text{O(II)}$  and  $\text{Ga}_{0.5}\text{Mn}_{0.5}\text{As(I,II)}$ . Only some of the systems show HM property, including  $\text{Zn}_{0.5}\text{Co}_{0.5}\text{O(I)}$  and  $\text{Zn}_{0.5}\text{Ni}_{0.5}\text{O(II)}$ . As shown in figure 2(c), there is a linear decrease in the ratio of  $c/a$  with increasing lattice constants of the substrate and the volume of the systems will be nearly conserved when they are relaxed completely to an equilibrium state under the biaxial strain. Meanwhile, our calculations showed that the AFM state of  $\text{Zn}_{0.5}\text{Co}_{0.5}\text{O(I)}$  could disappear at substrate lattice constants from 5.0 to 5.2 Å, and the system prefers the FM state in the range 5.2 Å–6.0 Å. The total magnetic moment of the system is  $6.0\mu_{\text{B}}/\text{cell}$  (cf figure 2(b)). Furthermore, from figure 2(e), the total density of states (TDOS) for majority spin and minority spin indicates that  $\text{Zn}_{0.5}\text{Co}_{0.5}\text{O(I)}$  ( $a = b = 5.6$  Å and  $c/a = 0.68$ ) clearly shows HM property with a SF gap of 0.6 eV. The SF gap reflects the position of the minority spin-conduction band minimum relative to the Fermi level of the majority spin. In other systems, such as

$\text{Zn}_{0.5}\text{Cr}_{0.5}\text{O(I,II)}$  and  $\text{Ga}_{0.5}\text{Mn}_{0.5}\text{As(I,II)}$ , they do not show HM property although the FM state is preferred in a certain range of substrate lattice constants. In figure 2(g), we can see that the calculated total magnetic moment of  $\text{Zn}_{0.5}\text{Cr}_{0.5}\text{O(I,II)}$  is close to  $7.8\mu_{\text{B}}/\text{cell}$ . The non-integer magnetic moment indicates that the systems of  $\text{Zn}_{0.5}\text{Cr}_{0.5}\text{O(I,II)}$  do not have HM property. Furthermore, the TDOS for majority spin and minority spin indicates that  $\text{Zn}_{0.5}\text{Cr}_{0.5}\text{O(I,II)}$  shows metallic property and not HM (cf figure 2(j)). The same magnetic and HM properties can be found in the system of  $\text{Zn}_{0.5}\text{Ni}_{0.5}\text{O(II)}$  (cf figures 3(h) and (l)).

The second group corresponds to the systems that always show FM coupling under the biaxial strain, i.e.  $\text{Zn}_{0.5}\text{Ni}_{0.5}\text{O(I)}$  and  $\text{Ga}_{0.5}\text{Cr}_{0.5}\text{As(I,II)}$ , but not all of them possess HM. For example, we can see clearly that  $\text{Ga}_{0.5}\text{Cr}_{0.5}\text{As(I,II)}$  always prefer the FM state when the substrate lattice constant changes from 5.0 to 6.8 Å (cf figure 3(a)). The calculated total magnetic moments of the system under the biaxial strain are always  $6.0\mu_{\text{B}}/\text{cell}$  except when the substrate constant is larger than  $a = b = 6.8$  Å (cf figure 3(b)). Figures 3(e) and (f) are the TDOS of  $\text{Ga}_{0.5}\text{Cr}_{0.5}\text{As(II)}$  corresponding to the substrate constants of 6.0 Å and 5.0 Å, respectively. Interestingly, the one at  $a = b = 6.0$  Å indicates HMF with a SF gap of 0.18 eV while the one at 5.0 Å does not possess HM property, although both systems prefer the FM state with a magnetization of  $6.0\mu_{\text{B}}/\text{cell}$ . As shown in figure 3(f),  $\text{Ga}_{0.5}\text{Cr}_{0.5}\text{As(II)}$  at 5.0 Å failed to exhibit the HM property because both the majority spin and minority spin show metallic property, in which the integer magnetic moment is a coincidence.  $\text{Zn}_{0.5}\text{Ni}_{0.5}\text{O(I)}$  always prefers the FM state with the energy difference  $\Delta E > 0$  independent of the substrate constants, and it provides a magnetic moment of  $4.0\mu_{\text{B}}/\text{cell}$  (cf figure 3(h)) with the HM property (cf figure 3(k)).

The third group corresponds to the systems that always show AFM states as the substrate changes including  $\text{Zn}_{0.5}\text{Mn}_{0.5}\text{O(I,II)}$ ,  $\text{Zn}_{0.5}\text{Fe}_{0.5}\text{O(I,II)}$ ,  $\text{Zn}_{0.5}\text{Co}_{0.5}\text{O(II)}$ ,  $\text{Ga}_{0.5}\text{Fe}_{0.5}\text{As(I,II)}$ ,  $\text{Ga}_{0.5}\text{Co}_{0.5}\text{As(I,II)}$  and  $\text{Ga}_{0.5}\text{Ni}_{0.5}\text{As(I,II)}$  (cf table 1). Their energy difference  $\Delta E$  is always negative, which reveals that the AFM state is more favoured than the FM one. All the GGA and GGA+ $U$  calculated magnetic properties are listed in table 2.

### 3.2. Magnetism described by the GGA + $U$ approach

At present, numerous theoretical studies have emerged on 3d impurities in oxides, using mostly the local-density approximations (LDA) or GGA in the frame of DFT. However, certain oxides such as ZnO or  $\text{In}_2\text{O}_3$  have a large electron affinity (low conduction band minimum energy) that is further exaggerated in LDA/GGA calculations where the notorious band-gap underestimation (e.g. in ZnO,  $E_{\text{g}} = 0.67$  eV in GGA compared with 3.4 eV in experiment) is mainly due to a very low energy of the conduction band minimum (CBM) [50]. The band-gap underestimation by GGA might affect the HM property in some systems, for example,  $\text{Zn}_{0.5}\text{Cr}_{0.5}\text{O(I,II)}$  and  $\text{Ga}_{0.5}\text{Mn}_{0.5}\text{As(I,II)}$ .

We adopt here a self-consistent band-gap correction by the GGA +  $U$  calculations. We find that the Zn-3d

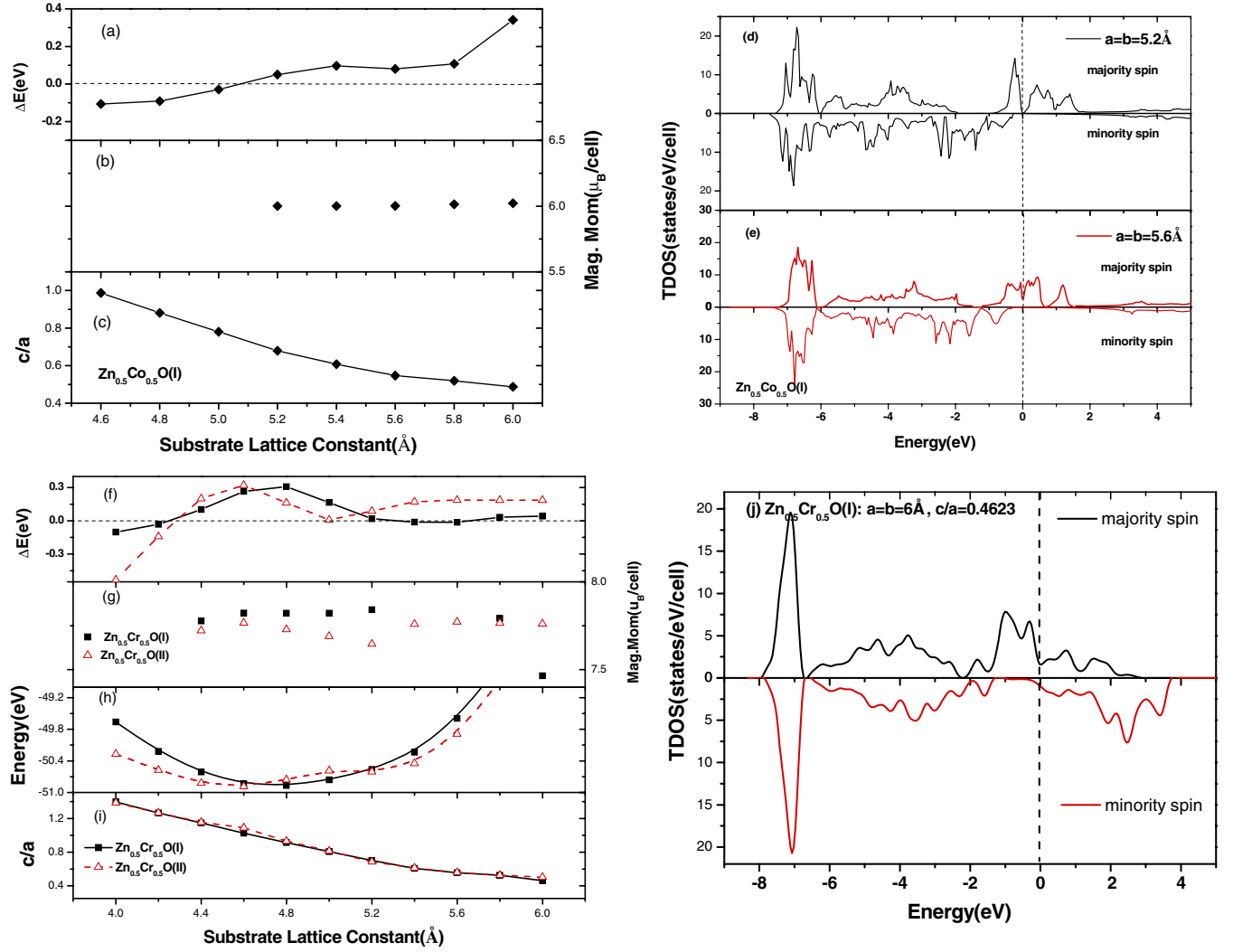


**Figure 2.** Plots of  $c/a$  (a), magnetic moments (b) and  $\Delta E$  (c) versus the substrate lattice constants for  $\text{Zn}_{0.5}\text{Co}_{0.5}\text{O(I)}$ , and the selected TDOS of  $\text{Zn}_{0.5}\text{Co}_{0.5}\text{O(I)}$  at  $a = b = 5.2$  Å (d) and 5.6 Å (e). The plots of  $\Delta E$  (f), magnetic moments (g), total energy (f) and  $c/a$  (i) versus the substrate lattice constants for  $\text{Zn}_{0.5}\text{Cr}_{0.5}\text{O(I,II)}$ , and the selected TDOS of  $\text{Zn}_{0.5}\text{Cr}_{0.5}\text{O(I)}$  at  $a = b = 6.0$  Å (j). Here the Fermi energy of TDOS is set to zero.

**Table 1.** Classification of the calculated systems: (I) systems undergo a transition between AFM and FM; (II) systems always show FM state; (III) systems always show AFM state.

I (AFM, FM)	II (FM)	III (AFM)
$\text{Zn}_{0.5}\text{Cr}_{0.5}\text{O(I, II)}$	$\text{Zn}_{0.5}\text{Ni}_{0.5}\text{O(I)}$	$\text{Zn}_{0.5}\text{Mn}_{0.5}\text{O(I,II)}$
$\text{Zn}_{0.5}\text{Co}_{0.5}\text{O(I)}$	$\text{Ga}_{0.5}\text{Cr}_{0.5}\text{As(I,II)}$	$\text{Zn}_{0.5}\text{Fe}_{0.5}\text{O(I,II)}$
$\text{Zn}_{0.5}\text{Ni}_{0.5}\text{O(II)}$		$\text{Zn}_{0.5}\text{Co}_{0.5}\text{O(II)}$
$\text{Ga}_{0.5}\text{Mn}_{0.5}\text{As(I,II)}$		$\text{Ga}_{0.5}\text{Fe}_{0.5}\text{As(I,II)}$
		$\text{Ga}_{0.5}\text{Co}_{0.5}\text{As(I,II)}$
		$\text{Ga}_{0.5}\text{Ni}_{0.5}\text{As(I,II)}$

has no contribution to the density of states near the Fermi level and the conducting bands for the systems favouring FM states. Similarly, in the systems of  $\text{Zn}_{0.5}\text{Ni}_{0.5}\text{O(I, II)}$  and  $\text{Zn}_{0.5}\text{Co}_{0.5}\text{O(I)}$  with HMF states, the Ni-3d and Co-3d density of states has no contribution for the TDOS near the Fermi energy level and the conducting band. Furthermore, we can find that the two systems ( $\text{Zn}_{0.5}\text{Cr}_{0.5}\text{O(I,II)}$  and  $\text{Ga}_{0.5}\text{Mn}_{0.5}\text{As(I,II)}$ ) prefer FM without HM property from the

GGA calculated results. Thus, we employ the corrections on these two systems with GGA +  $U$ . We use  $U = 3.5$  eV, 4.0 eV and 4.5 eV for Cr in  $\text{Zn}_{0.5}\text{Cr}_{0.5}\text{O(I,II)}$  and  $U = 2.5$  eV, 3.0 eV and 3.5 eV for Mn in  $\text{Ga}_{0.5}\text{Mn}_{0.5}\text{As(I,II)}$ , respectively, to investigate the effect of  $U$  correction on the HM property of these systems, where  $U$  is an efficient value ( $U_{\text{eff}} = U - J$ ).

Figures 4(a)–(l) show the TDOS as a function of  $U$  for  $\text{Zn}_{0.5}\text{Cr}_{0.5}\text{O(I,II)}$  and  $\text{Ga}_{0.5}\text{Mn}_{0.5}\text{As(I,II)}$ . As the  $U$  value increases, the peak of TDOS is pushed deeper into the valence band in these four systems. This is due to the fact that the energy separating the Cr (Mn) d levels and the dangling bond levels increases with  $U$ . As a result, the effective coupling between Cr(Mn) and the host-like states decreases. The calculated total magnetic moment is  $8.0\mu_B/\text{cell}$  for  $\text{Zn}_{0.5}\text{Cr}_{0.5}\text{O(I,II)}$  and  $\text{Ga}_{0.5}\text{Mn}_{0.5}\text{As(I,II)}$  using GGA +  $U$  (cf table 2). As shown in figures 4(a)–(c) and (d)–(f), it is clear that the majority spin bands are metallic, but there is a wide gap around the Fermi level for the minority spin. As shown in figures 4(a)–(c), we can see that the SF

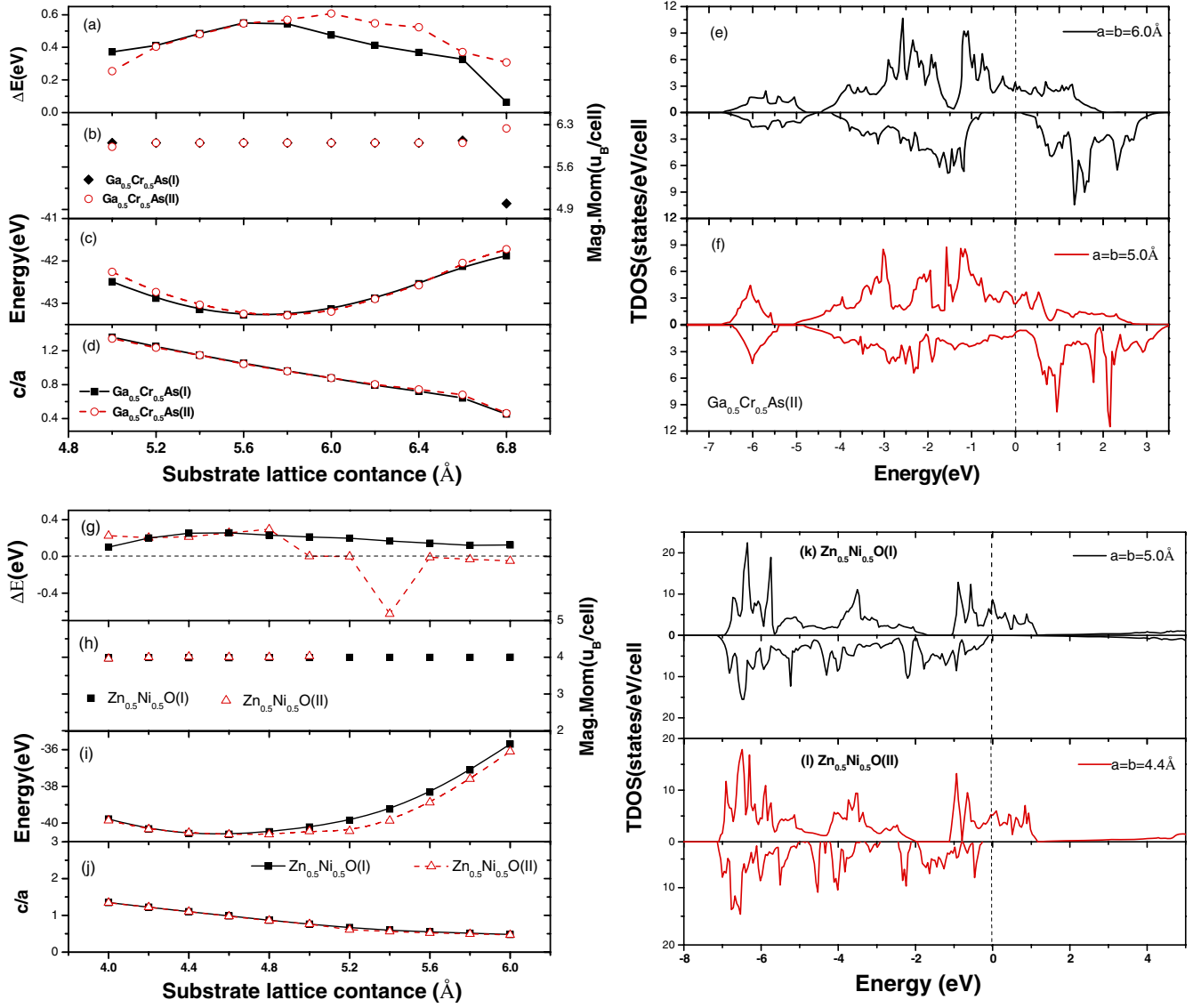


**Figure 3.** Plots of  $\Delta E$  (a), (g), magnetization (b), (h), total energy (c), (i) and  $c/a$  (d), (j) versus the substrate lattice constants for  $\text{Ga}_{0.5}\text{Cr}_{0.5}\text{As}$ (I,II) and  $\text{Zn}_{0.5}\text{Ni}_{0.5}\text{O}$ (I,II), the TDOS of  $\text{Ga}_{0.5}\text{Cr}_{0.5}\text{As}$ (II) at  $a = b = 6.0 \text{ \AA}$  (e) and  $5.0 \text{ \AA}$  (f); as well as the TDOS of  $\text{Zn}_{0.5}\text{Ni}_{0.5}\text{O}$ (I) (k) at  $a = b = 5.0 \text{ \AA}$  and  $\text{Zn}_{0.5}\text{Ni}_{0.5}\text{O}$ (II) (l) at  $a = b = 4.4 \text{ \AA}$ .

**Table 2.** The GGA and GGA +  $U$  calculated magnetic properties with respect to the substrate lattice constants for the ternary alloy TM–ZnO and TM–GaAs (TM = Cr, Mn, Fe, Co, Ni).

Compound	$a = b$ (Å) (FM)	$a = b$ (Å) (AFM)	M(GGA) ( $\mu_B$ /cell)	HM (GGA)	M(GGA + $U$ ) ( $\mu_B$ /cell)	HM (GGA + $U$ )
$\text{Zn}_{0.5}\text{Cr}_{0.5}\text{O}$ (I)	4.4–5.2 and 5.6–6.0	4.0–4.2 and 5.4	7.5–7.8	Nearly	8.0	Yes
$\text{Zn}_{0.5}\text{Cr}_{0.5}\text{O}$ (II)	4.4–6.0	4.0–4.2	7.6–7.8	Nearly	8.0	Yes
$\text{Zn}_{0.5}\text{Mn}_{0.5}\text{O}$ (I,II)	—	4.0–6.0	—	—	—	—
$\text{Zn}_{0.5}\text{Fe}_{0.5}\text{O}$ (I,II)	—	4.0–6.0	—	—	—	—
$\text{Zn}_{0.5}\text{Co}_{0.5}\text{O}$ (I)	5.2–6.0	4.0–5.0	6.0	Yes	—	—
$\text{Zn}_{0.5}\text{Co}_{0.5}\text{O}$ (II)	—	4.0–6.0	—	—	—	—
$\text{Zn}_{0.5}\text{Ni}_{0.5}\text{O}$ (I)	4.0–6.0	—	4.0	Yes	—	—
$\text{Zn}_{0.5}\text{Ni}_{0.5}\text{O}$ (II)	4.0–5.0	5.2–6.0	4.0	Yes	—	—
$\text{Ga}_{0.5}\text{Cr}_{0.5}\text{As}$ (I,II)	5.0–6.8	—	6.0	Yes	—	—
$\text{Ga}_{0.5}\text{Mn}_{0.5}\text{As}$ (I)	5.4–6.4	5.0–5.2 and 6.6–6.8	7.8–7.9	No	8.0	Yes
$\text{Ga}_{0.5}\text{Mn}_{0.5}\text{As}$ (II)	5.2–6 and 6.4–6.8	5.0, 6.2	7.2–7.9	No	8.0	Yes
$\text{Ga}_{0.5}\text{Fe}_{0.5}\text{As}$ (I,II)	—	5.0–6.8	—	—	—	—
$\text{Ga}_{0.5}\text{Co}_{0.5}\text{As}$ (I,II)	—	5.0–6.8	—	—	—	—
$\text{Ga}_{0.5}\text{Ni}_{0.5}\text{As}$ (I,II)	—	5.0–6.8	—	—	—	—

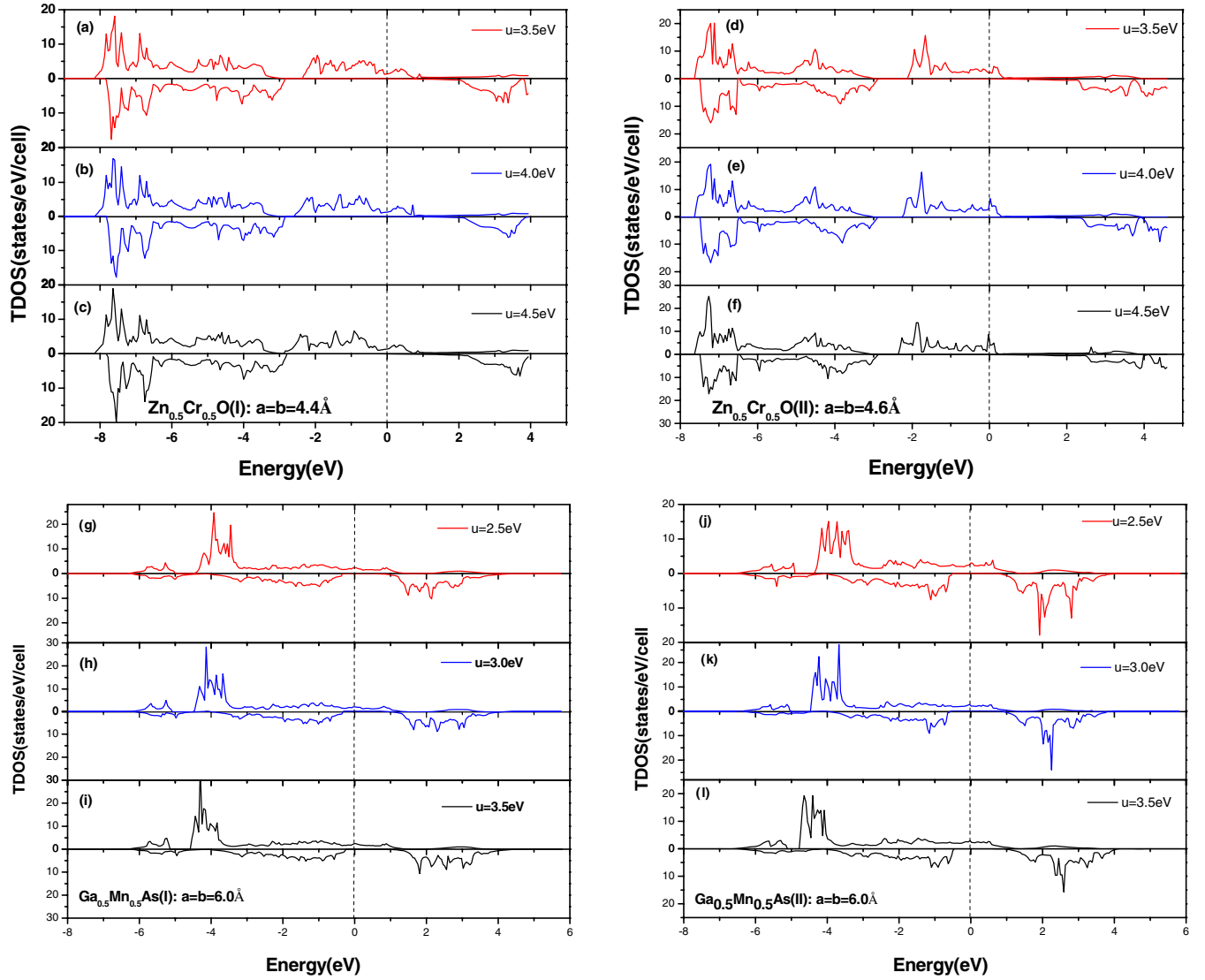


**Figure 4.** Plots of the TDOS of  $\text{Zn}_{0.5}\text{Cr}_{0.5}\text{O(I)}$  at  $a = b = 4.4 \text{ \AA}$  and of  $\text{Zn}_{0.5}\text{Cr}_{0.5}\text{O(II)}$  at  $a = b = 4.6 \text{ \AA}$  with  $U = 3.5 \text{ eV}$ ,  $4.0 \text{ eV}$  and  $4.5 \text{ eV}$  are shown in (a)–(f), respectively, and the TDOS of  $\text{Ga}_{0.5}\text{Mn}_{0.5}\text{As(I)}$  and  $\text{Ga}_{0.5}\text{Mn}_{0.5}\text{As(II)}$  at  $a = b = 6.0 \text{ \AA}$  with  $U = 2.5 \text{ eV}$ ,  $3.0 \text{ eV}$  and  $3.5 \text{ eV}$  are shown in (g)–(l).

gaps are  $2.0 \text{ eV}$ ,  $2.1 \text{ eV}$  and  $2.2 \text{ eV}$  for  $U = 3.5$ ,  $4.0$  and  $4.5 \text{ eV}$ , respectively. This indicates that the system is a robust HMF. Similarly,  $\text{Zn}_{0.5}\text{Cr}_{0.5}\text{O(II)}$  is also shown to be a robust HMF (cf figures 4(d)–(f)).

Figures 4(g)–(l) show the TDOS of  $\text{Ga}_{0.5}\text{Mn}_{0.5}\text{As(I)}$  ( $a = b = 6.0 \text{ \AA}$ ,  $c/a = 0.8836$ ) and  $\text{Ga}_{0.5}\text{Mn}_{0.5}\text{As(II)}$  ( $a = b = 6.0 \text{ \AA}$ ,  $c/a = 0.8969$ ) with  $U = 2.5 \text{ eV}$ ,  $3.0 \text{ eV}$  and  $3.5 \text{ eV}$ , respectively. It is obvious that the majority spin bands are metallic, while there is a band gap of  $1.2 \text{ eV}$ ,  $1.3 \text{ eV}$  and  $1.4 \text{ eV}$  for  $\text{Ga}_{0.5}\text{Mn}_{0.5}\text{As(I)}$  ( $a = b = 6.0 \text{ \AA}$ ,  $c/a = 0.8836$ ), and  $1.3 \text{ eV}$ ,  $1.5 \text{ eV}$  and  $1.5 \text{ eV}$  for  $\text{Ga}_{0.5}\text{Mn}_{0.5}\text{As(II)}$  ( $a = b = 6.0 \text{ \AA}$ ,  $c/a = 0.8969$ ) with  $U = 2.5 \text{ eV}$ ,  $3.0 \text{ eV}$  and  $3.5 \text{ eV}$  around the Fermi level for minority spin, respectively. As shown in figures 4(g)–(i), the SF gaps are  $0.9 \text{ eV}$ ,  $1.1 \text{ eV}$  and  $1.2 \text{ eV}$  for  $\text{Ga}_{0.5}\text{Mn}_{0.5}\text{As(I)}$  ( $a = b = 6.0 \text{ \AA}$ ,  $c/a = 0.8836$ ) with  $U = 2.5 \text{ eV}$ ,  $3.0 \text{ eV}$  and  $3.5 \text{ eV}$ , respectively. For  $\text{Ga}_{0.5}\text{Mn}_{0.5}\text{As(II)}$  ( $a = b = 6.0 \text{ \AA}$ ,  $c/a = 0.8836$ ), the SF gaps are  $0.85 \text{ eV}$ ,  $0.95 \text{ eV}$  and  $1.05 \text{ eV}$  for  $U = 2.5 \text{ eV}$ ,  $3.0 \text{ eV}$  and  $3.5 \text{ eV}$ , as shown in figures 4(j)–(l). Thus, with the

correction of GGA+ $U$ , we find that HMF may be available in  $\text{Zn}_{0.5}\text{Cr}_{0.5}\text{O(I,II)}$  and  $\text{Ga}_{0.5}\text{Mn}_{0.5}\text{As(I,II)}$  although they are not predicted by GGA calculations.

#### 4. Summary

We have investigated the basic electronic structure, magnetic and half-metallic properties of TM-alloyed ZnO and GaAs (TM = Cr, Mn, Fe, Co, Ni) thin films with a concentration of 50% using GGA and GGA +  $U$  calculations. The magnetic state of these systems often strongly depends on the biaxial strain.  $\text{Zn}_{0.5}\text{Co}_{0.5}\text{O(I)}$ ,  $\text{Zn}_{0.5}\text{Ni}_{0.5}\text{O(I,II)}$  and  $\text{Ga}_{0.5}\text{Cr}_{0.5}\text{As(I,II)}$  are found to be HMFs according to the 0 calculations. Using GGA +  $U$ , we further find that  $\text{Zn}_{0.5}\text{Cr}_{0.5}\text{O(I,II)}$  and  $\text{Ga}_{0.5}\text{Mn}_{0.5}\text{As(I,II)}$  also show robust HM property. This study provides a general picture of the magnetic and HM properties of TM-alloyed ZnO and GaAs thin films, which is helpful in exploring HMFs. For example, on the substrate of Si (lattice constant of  $5.42 \text{ \AA}$ ), Cr-alloyed GaAs(I), Mn-alloyed

GaAs(II) or Cr-alloyed ZnO(II) are suggested for potential HMFs according to our predictions.

## Acknowledgments

We are grateful for the computer time at the High Performance Computer Center of Shenzhen Institute of Advanced Technology (SIAT), Chinese Academy of Science and the High Performance Grid Computer Center (SCUTGrid) of South China University of Technology. This work was supported by NSFC under Grant No 10704025, the Key Project of Chinese Ministry of Education (Grant No 108105) and the New Century Excellent Talents Program (Grant No NCET-08-0202).

## References

- [1] Zutic I, Fabian J and Das Sarma S 2004 *Rev. Mod. Phys.* **76** 323
- [2] Pan F, Song C, Liu X J, Yang Y C and Zeng F 2008 *Mater. Sci. Eng. R* **62** 1
- [3] Qiu M D, Yao Z H, Wei Z R, Zhai Y Q, Tian S and Zhang S 2009 *Spectrosc. Spectral Anal.* **29** 277
- [4] Dietl T, Ohno H, Matsukura F, Cibert J and Ferrand D 2000 *Science* **287** 1019
- [5] Sato K and Katayama-Yoshida H 2000 *Japan. J. Appl. Phys. Part 2* **39** L555
- [6] Zhao Y J, Geng W T, Freeman A J and Delley B 2002 *Phys. Rev. B* **65** 113202
- [7] Pask J E, Yang L H, Fong C Y, Pickett W E and Dag S 2003 *Phys. Rev. B* **67** 224420
- [8] Xie W H, Liu B G and Pettifor D G 2003 *Phys. Rev. B* **68** 134407
- [9] Galanakis I 2010 *J. Comput. Theor. Nanosci.* **7** 474
- [10] Sakamaki M, Konishi T and Ohta Y 2009 *Phys. Rev. B* **80** 024416
- [11] Shimizu D, Kobori H, Yamasaki A, Sugimura A, Taniguchi T, Kawanaka H, Ando A and Shimizu T 2008 *Magn. Mater.* **1003** 19
- [12] Balke B, Ouardi S, Graf T, Barth J, Blum C G F, Fecher G H, Shkabrko A, Weidenkaff A and Felser C 2010 *Solid State Commun.* **150** 529
- [13] Mansell R, Laloe J B, Holmes S N, Wong P K J, Xu Y B, Farrer I, Jones G A C, Ritchie D A and Barnes C H W 2010 *J. Appl. Phys.* **108** 034507
- [14] Ahmadian F, Abolhassani M R, Hashemifar S J and Elahi M 2010 *J. Magn. Magn. Mater.* **322** 1004
- [15] Davies R P, Abernathy C R, Pearton S J, Norton D P, Ivill M P and Ren F 2009 *Chem. Eng. Commun.* **196** 1030
- [16] Reed M L, El-Masry N A, Stadelmaier H H, Ritums M K, Reed M J, Parker C A, Roberts J C and Bedair S M 2001 *Appl. Phys. Lett.* **79** 3473
- [17] Park S E, Lee H J, Cho Y C, Jeong S Y, Cho C R and Cho S 2002 *Appl. Phys. Lett.* **80** 4187
- [18] Fukumura T, Jin Z W, Kawasaki M, Shono T, Hasegawa T, Koshihara S and Koinuma H 2001 *Appl. Phys. Lett.* **78** 958
- [19] Pearton S J, Abernathy C R, Norton D P, Hebard A F, Park Y D, Boatner L A and Budai J D 2003 *Mater. Sci. Eng. R* **40** 137
- [20] Macdonald A H, Schiffer P and Samarth N 2005 *Nature Mater.* **4** 195
- [21] Zunger A, Lany S and Raebiger H 2010 *Physics* **3** 53
- [22] Miao M S and Lambrecht W R L 2005 *Phys. Rev. B* **72** 64409
- [23] Zhao Y J and Zunger A 2005 *Phys. Rev. B* **71** 132403
- [24] Mavropoulos P and Galanakis I 2007 *J. Phys.: Condens. Matter* **19** 315221
- [25] Miao M S and Lambrecht W R L 2005 *Phys. Rev. B* **71** 064407
- [26] Xie W H, Xu Y Q, Liu B G and Pettifor D G 2003 *Phys. Rev. Lett.* **91** 037204
- [27] Sanyal B, Bergqvist L and Eriksson O 2003 *Phys. Rev. B* **68** 054417
- [28] Huang D, Zhao Y J, Chen L J, Chen D H and Shao Y Z 2008 *J. Appl. Phys.* **104** 053709
- [29] Zhang S L, Wang W, Zhang E H and Xiao W 2010 *Phys. Lett. A* **374** 3234
- [30] Ono K, Okabayashi J, Mizuguchi M, Oshima M, Fujimori A and Akinaga H 2002 *J. Appl. Phys.* **91** 8088
- [31] Bi J F, Zhao J H, Deng J J, Zheng Y H, Li S S, Wu X G and Jia Q J 2006 *Appl. Phys. Lett.* **88** 142509
- [32] Zhao J H, Matsukura F, Takamura K, Abe E, Chiba D and Ohno H 2001 *Appl. Phys. Lett.* **79** 2776
- [33] Nazmul A M, Sugahara S and Tanaka M 2003 *Phys. Rev. B* **67** 241308
- [34] Nazmul A M, Sugahara S and Tanaka M 2002 *Appl. Phys. Lett.* **80** 3120
- [35] Nazmul A M, Sugahara S and Tanaka M 2003 *J. Cryst. Growth* **251** 303
- [36] Mack S, Myers R C, Heron J T, Gossard A C and Awschaloma D D 2008 *Appl. Phys. Lett.* **92** 192502
- [37] Ihm J, Zunger A and Cohen M L 1979 *J. Phys. C: Solid State Phys.* **12** 4409
- [38] Perdew J P and Wang Y 1992 *Phys. Rev. B* **45** 13244
- [39] Kresse G and Hafner J 1993 *Phys. Rev. B* **47** 558
- [40] Kresse G and Furthmüller J 1996 *Phys. Rev. B* **54** 11169
- [41] Monkhorst H J and Pack J D 1976 *Phys. Rev. B* **13** 5188
- [42] Anisimov V I, Zaanen J and Andersen O K 1991 *Phys. Rev. B* **44** 943
- [43] Anisimov V I, Solovyev I V and Korotin M A 1993 *Phys. Rev. B* **48** 16929
- [44] Solovyev I V, Dederichs P H and Anisimov V I 1994 *Phys. Rev. B* **50** 16861
- [45] Gopal P and Spaldin N A 2006 *Phys. Rev. B* **74** 094418
- [46] Lany S, Raebiger H and Zunger A 2008 *Phys. Rev. B* **77** 241201
- [47] Mahadevan P and Zunger A 2004 *Phys. Rev. B* **69** 115211
- [48] Mahadevan P, Zunger A and Sarma D D 2004 *Phys. Rev. Lett.* **93** 177201
- [49] Deng J J, Zhao J H, Bi J F, Niu Z C, Yang F H, Wu X G and Zheng H Z 2006 *J. Appl. Phys.* **99** 093902
- [50] Usuda M, Hamada N, Kotani T and van Schilfhaarde M 2002 *Phys. Rev. B* **66** 125101
- [51] Brozél M R and Stillman G E (ed) 1996 *Properties of Gallium Arsenide* 3rd edn (London: INSPEC) p 501